

Article

A Modified Osprey Optimization Algorithm for Solving Global Optimization and Engineering Optimization Design Problems

Liping Zhou ¹, Xu Liu ^{2,*}, Ruiqing Tian ³, Wuqi Wang ¹ and Guowei Jin ¹

¹ College of Emergency Technology, Zhejiang College of Security Technology, No. 2555 Ouhai Avenue, Ouhai District, Wenzhou 325016, China; zhouliping0814@126.com (L.Z.); wangwuqi1977@126.com (W.W.); jinguowei1989@126.com (G.J.)

² Postdoctoral Rover, Shanghai University of Finance and Economics, No. 777 Guoding Road, Yangpu District, Shanghai 200433, China

³ College of New Energy Equipment, Zhejiang College of Security Technology, No. 2555 Ouhai Avenue, Ouhai District, Wenzhou 325016, China; trq_work@outlook.com

* Correspondence: liuxu@mail.shufe.edu.cn

Abstract: The osprey optimization algorithm (OOA) is a metaheuristic algorithm with a simple framework, which is inspired by the hunting process of ospreys. To enhance its searching capabilities and overcome the drawbacks of susceptibility to local optima and slow convergence speed, this paper proposes a modified osprey optimization algorithm (MOOA) by integrating multiple advanced strategies, including a Lévy flight strategy, a Brownian motion strategy and an RFDB selection method. The Lévy flight strategy and Brownian motion strategy are used to enhance the algorithm's exploration ability. The RFDB selection method is conducive to search for the global optimal solution, which is a symmetrical strategy. Two sets of benchmark functions from CEC2017 and CEC2022 are employed to evaluate the optimization performance of the proposed method. By comparing with eight other optimization algorithms, the experimental results show that the MOOA has significant improvements in solution accuracy, stability, and convergence speed. Moreover, the efficacy of the MOOA in tackling real-world optimization problems is demonstrated using five engineering optimization design problems. Therefore, the MOOA has the potential to solve real-world complex optimization problems more effectively.



Citation: Zhou, L.; Liu, X.; Tian, R.; Wang, W.; Jin, G. A Modified Osprey Optimization Algorithm for Solving Global Optimization and Engineering Optimization Design Problems. *Symmetry* **2024**, *16*, 1173. <https://doi.org/10.3390/sym16091173>

Academic Editor: Theodore E. Simos

Received: 14 August 2024

Revised: 1 September 2024

Accepted: 2 September 2024

Published: 6 September 2024



Copyright: © 2024 by the authors. Licensee MDPI, Basel, Switzerland. This article is an open access article distributed under the terms and conditions of the Creative Commons Attribution (CC BY) license (<https://creativecommons.org/licenses/by/4.0/>).

1. Introduction

The optimization problems exist in various fields, such as engineering design [1], resource allocation [2], scheduling and routing [3], image segmentation [4], machine learning and data mining [5]. However, finding the global optimum of complex and dynamic problems can be computationally expensive or even impossible for the traditional optimization methods, such as gradient-based techniques [6], and Newton's method [7]. In the last few decades, various metaheuristic algorithms (MAs) have been developed to tackle challenging optimization problems. The metaheuristic algorithm is one type of population-based optimization method that has the merits of flexibility and simplicity and is gradient-free [8–10].

In each metaheuristic algorithm, exploration (global) and exploitation (local) searches are two crucial processes for achieving the optimal solution. In the early stage of iterations, the exploration search is emphasized to guarantee the algorithm widely explores the search space for global optimum, while the exploitation search is desired in the later stage to improve the quality of the obtained optimal solution. However, it is a challenging task to strike a balance between the global search and local search. Motivated by the no free lunch (NFL) theorem [11], which states there is no optimization algorithm that can solve

all optimization issues, it is always needed to develop new optimizers to address newly appeared optimization problems.

Some well-known and newly proposed optimizers are listed in Table 1, which are sorted into four groups: swarm-based, physics/mathematics/chemistry-based, human-based, and plant-based. In the swarm-based methods, particle swarm optimization (PSO) is a famous algorithm that was proposed in 1995 [8] and was inspired by the foraging behaviors of flying birds. The greater cane rat algorithm (GCRA) [12] is the newest developed algorithm that is motivated by the foraging and mating behaviors of cane rats. The physics/mathematics/chemistry-based algorithms are those approaches that are inspired by the laws or principles of physics, mathematics, and chemistry, such as optics-inspired optimization (OIO) [13], the artificial electric field algorithm (AEFA) [14], the Archimedes optimization algorithm (AOA) [10], and the material generation algorithm (MGA) [15]. The human-based category is another representative collection of metaheuristic algorithms, which are inspired by the intelligent social behaviors of human beings, including school-based optimization (SBO) [16], political optimizer (PO) [17], and the special forces algorithm (SFA) [18]. The last class is the plant-based methods. As its name implies, these methods usually simulate the group behavior of plants in nature, such as the carnivorous plant algorithm (CPA) [19], the dandelion optimizer (DO) [20], and the orchard algorithm (OA) [21]. Other categories of MAs also include evolutionary-based algorithms, such as the genetic algorithm (GA) [22] and differential evolution (DE) [23].

Table 1. A summary of advanced metaheuristic algorithms.

Category	Algorithm Name	Year	Inspiration	Application	Reference
Swarm-based	Particle swarm optimization (PSO)	1995	The foraging behaviors of birds	Multilayer perceptron	[8]
	Grey wolf optimization (GWO)	2014	Hierarchy of Grey wolf behavior	29 benchmark functions, three engineering design problems, optical buffer design	[9]
	Fire Hawk Optimizer (FHO)	2022	Foraging behavior of whistling kites, black kites, and brown falcons	CEC2020, mechanical engineering design problems	[24]
	Osprey optimization algorithm (OOA)	2023	The hunting fish process of osprey	CEC2017, CEC2011 test suite	[25]
	Spider wasp optimizer (SWO)	2023	Behaviors of the female spider wasps	CEC2005, CEC2014, CEC2017, CEC2020, engineering design problems, photovoltaic models	[26]
Physics/mathematics/chemistry-based	Greater cane rat algorithm (GCRA)	2024	Foraging and mating behaviors of cane rats in nature	22 classical benchmark functions, 10 CEC2020 functions, CEC2011 real-world problems	[12]
	Optics-inspired optimization (OIO)	2015	Law of reflection	CEC2005, bi-objective optimization of centrifuge pumps	[13]
	Artificial electric field algorithm (AEFA)	2019	Coulomb's law of electrostatic force	CEC2015	[14]
	Archimedes optimization algorithm (AOA)	2021	Classical Archimedes's principle	CEC2005, 5 engineering design problems	[10]
	Material generation algorithm (MGA)	2021	Chemical compounds and reactions in producing new materials	CEC2017, 15 engineering design problems	[15]
Human-based	School-Based Optimization (SBO)	2018	Traditional educational process that operates within a multi-classroom school	Design of structural steel frames	[16]
	Political optimizer (PO)	2020	Multi-phased process of politics	50 benchmark functions and 4 constrained engineering design problems	[17]
	Special forces algorithm (SFA)	2023	Missions of modern special forces	CEC2005, engineering design problems	[18]
Plant-based	Carnivorous plant algorithm (CPA)	2021	Carnivorous plants adapting to survive in the harsh environment	CEC2017, mechanical engineering design problems, controlling the orientation of robotic arm	[19]
	Dandelion optimizer (DO)	2022	Process of dandelion seed long-distance flight relying on wind	CEC2017 and 4 real-world optimization problems	[20]
	Orchard algorithm (OA)	2023	Fruit gardening process	60 test functions, 5 engineering benchmark problems	[21]

The osprey optimization algorithm (OOA) is a new swarm-based intelligence algorithm that was developed in 2023 [25]. OOA is inspired by the hunting process of natural ospreys, including two phases of hunting the fish and carrying fish to a suitable position. Experiments on the CEC2017 test suite and twenty-two real-world optimization problems were conducted to evaluate the optimization performance of OOA. Compared to twelve well-known algorithms, the results demonstrate that OOA has adequate performance in solving these problems. Moreover, the OOA also displays superior performance in solving the economic load dispatch (ELD) problem [27]. However, like other approaches, OOA may face the problems of insufficient global exploration, slow convergence, and local optima when solving challenging optimization problems. To overcome the potential shortcomings of the original OOA, this paper proposes a modified osprey optimization algorithm (MOOA), which combines three advanced strategies. The main contributions of this paper are listed as follows:

- The Lévy flight strategy is employed to help OOA jump out of local minima and strengthen its global search capability.
- The Brownian motion strategy is introduced in Phase 1 of OOA to enable the individuals to explore the promising regions.
- The RFDB selection method is used to select a high-potential solution candidate in Phase 2 of OOA.
- The superior performance of the proposed MOOA is verified by comparing other advanced algorithms according to the numerical results, convergence curves and box plots of CEC2017 and CEC2022 test functions.
- The results of five practical engineering optimization problems also demonstrate the effectiveness of the MOOA.

The remaining sections are structured as follows: Section 2 presents the standard osprey optimization algorithm. Then, the improvements of the osprey optimization algorithm and the proposed MOOA are provided in Section 3. Section 4 is the experimental results of benchmark functions for the proposed algorithm and other compared state-of-the-art methods. The application of the proposed algorithm to real-world problems is further discussed in Section 5. At last, Section 6 summarizes the presented work and provides some suggestions for future research.

2. Osprey Optimization Algorithm

2.1. Inspiration

The osprey optimization algorithm (OOA) [25] is inspired by the natural hunting behaviors of osprey, including identifying the fish's position, hunting fish, and carrying the fish. In OOA, the behavior of hunting fish is mathematically modeled as the exploration phase, and the behavior of carrying fish is formulated as the exploitation phase. This framework enables OOA to balance exploration and exploitation and obtain the optimal solution of optimization problems. The details of OOA are given as follows.

2.2. Mathematical Modeling

In OOA, like other metaheuristic algorithms, the positions of all ospreys are randomly generated within the search space by using Equation (1).

$$X_{i,j} = \text{rand} \times (ub_j - lb_j) + lb_j, j = 1, 2, \dots, D \quad (1)$$

where rand is the random number between 0 and 1, and ub_j and lb_j are the upper bound and lower bound of the search space. D is the dimension of the optimization problem. And $X_{i,j}$ is the generated position of the i -th individual in the j -th dimension.

Furthermore, in the iterative process, two phases are designed in the OOA, i.e., hunting the fish and carrying the fish, which are introduced below.

2.2.1. Phase 1: Exploring the Search Space and Hunting the Fish

The first stage of OOA is to perform the global search and avoid falling into local optima. In this phase, ospreys attack fishes and try to explore the entire search space. At first, the fishes' positions are determined using Equation (2).

$$FP_i = \{X_k | k \in \{1, 2, \dots, N\} \cap F_k < F_i\} \cup \{X_{best}\} \quad (2)$$

where FP_i is the selected position of fish for the i -th osprey. F_i is the fitness of the i -th individual. X_{best} means the position of the best individual.

After identifying the positions of fishes, osprey will try to attack these targets, which is mathematically modeled in Equation (3).

$$X_{i,j}^{P1} = X_{i,j} + r_1 \times (SF_{i,j} - I_{i,j} \times X_{i,j}), i = 1, 2, \dots, N, j = 1, 2, \dots, D \quad (3)$$

where r_1 is a random number within $[0, 1]$. $SF_{i,j}$ is the position of fish, which is selected from the identified fishes. $I_{i,j}$ is a random integer within $\{1, 2\}$. Then, the new position will replace the previous position if its fitness is better than the previous value, which is defined in Equation (4).

$$X_i = \begin{cases} X_i^{P1}, & \text{if } F_i^{P1} < F_i \\ X_i, & \text{otherwise} \end{cases} \quad (4)$$

where F_i^{P1} is the fitness of the newly generated position.

2.2.2. Phase 2: Exploiting the Search Space and Carrying the Fish

In the second phase, ospreys need to find a suitable position after hunting a fish. This stage makes the OOA perform a local search and converge to the optimal solution. The mathematical model is shown in Equation (5).

$$X_{i,j}^{P2} = X_{i,j} + \frac{lb_j + r_2 \times (ub_j - lb_j)}{t}, t = 1, 2, \dots, T \quad (5)$$

where lb_j and ub_j are the lower and upper boundaries of the search space. r_2 is a random value within $[0, 1]$. t and T are the current and maximum iteration number, respectively. Then, like in the previous phase, a better solution will be adopted by the new individual, which is determined using Equation (6).

$$X_i = \begin{cases} X_i^{P2}, & \text{if } F_i^{P2} < F_i \\ X_i, & \text{otherwise} \end{cases} \quad (6)$$

where F_i^{P2} is the fitness of the newly generated position.

The flowchart and pseudocode of OOA are shown in Figure 1 and Algorithm 1.

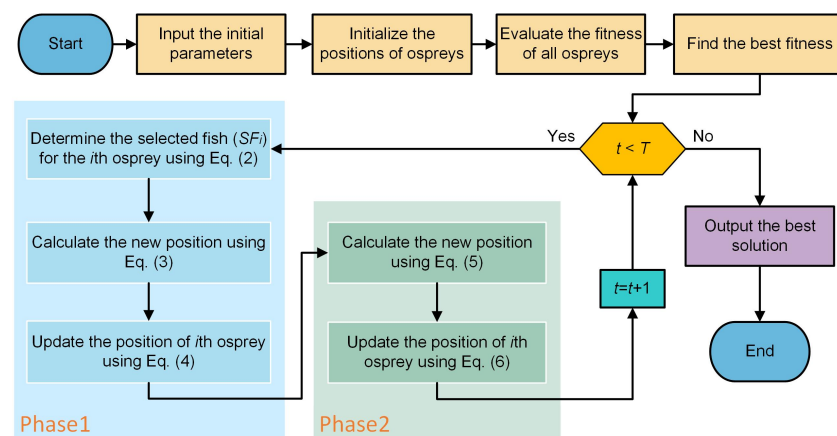


Figure 1. The flowchart of OOA.

Algorithm 1 The pseudocode of OOA.

```

1: Input the population size ( $N$ ) and maximum iterations ( $T$ ).
2: Initialize the positions of all ospreys using Equation 1.
3: for  $t = 1$  to  $T$  do
4:   for  $i = 1$  to  $N$  do
5:     Phase 1: Exploring the search space and hunting the fish
6:     Determine the position of fish using Equation (2).
7:     Calculate the new position of osprey using Equation (3).
8:     Check the boundary conditions and update the  $i$ -th osprey using Equation (4).
9:     Phase 2: Exploiting the search space and carrying the fish
10:    Calculate the new position of osprey using Equation (5).
11:    Check the boundary conditions and update the  $i$ -th osprey using Equation (6).
12:   end for
13: end for
14: Output the best solution.

```

3. Proposed MOOA Approach

3.1. Shortcomings of OOA

In the standard OOA, two natural behaviors of ospreys are mathematically modeled, i.e., hunting the fish in the selected location and carrying the fish to a suitable position. Although OOA has shown superior performance in some optimization problems, it still has the possibility of falling into local optima and weak exploitative abilities when solving other types of optimization problems and failing to obtain optimal solutions on more complex and high-dimensional problems. Thus, OOA still needs to be further improved.

3.2. Modified Methods

In this work, three improvements are applied to the basic OOA to enhance its global search capabilities and accelerate convergence speed. These improvements are the Lévy flight strategy, the Brownian motion strategy and the RFDB selection method. The details are shown below.

3.2.1. Lévy Flight Strategy

In the global search process of OOA, parameter r_1 limits the search area of the ospreys, which needs to be modified. The Lévy flight strategy (LFS) is an effective method to help optimization algorithms escape local minima [28]. The Lévy flight value is calculated as follows:

$$Levy(1) = \frac{u}{|v|^{\frac{1}{\beta}}} \quad (7)$$

$$\sigma_u = \left(\frac{\Gamma(1 + \beta) \times \sin(\frac{\pi\beta}{2})}{\Gamma(\frac{1+\beta}{2}) \times \beta \times 2^{(\frac{\beta-1}{2})}} \right)^{\frac{1}{\beta}} \quad (8)$$

where u and v satisfy the Gaussian distribution, $u \sim (0, \sigma_u^2)$, $v \sim (0, \sigma_v^2)$, $\sigma_v = 1$, $\beta = 1.5$, and Γ is the standard gamma function.

In the MOOA, the Lévy flight strategy is applied to replace the random number r_1 in Equation (3). The new equation of hunting fish is modified in Equation (9).

$$X_{i,j}^{P1} = X_{i,j} + Levy(1) \times (SF_{i,j} - I_{i,j} \times x_{i,j}) \quad (9)$$

3.2.2. Brownian Motion Strategy

To increase the diversity of the population, the Brownian motion strategy (BMS) is applied in Phase 1 of OOA as another choice for hunting the fish. This strategy comes from the Brownian movement of predators in MPA [29], which is a probabilistic exploration method and enables the individuals to explore promising regions. Thus, it can help the ospreys search the entire space more efficiently. The modified equation is presented as follows:

$$X_{i,j}^{P1} = X_{i,j} + P \times CF \times randn \times (randn \times SF_{i,j} - I_{i,j} \times x_{i,j}) \quad (10)$$

$$CF = (1 - \frac{t}{T})^{(2 \times t/T)} \quad (11)$$

where P is a constant value set to 0.5. $randn$ is a random number satisfying the standard normal distribution.

3.2.3. RFDB Selection Method

To improve the exploitation ability of OOA, the roulette fitness–distance balance-based (RFDB) selection method is employed in Phase 2 of OOA [30]. The RFDB selection method considers both the fitness and distance values of individuals. Thus both the fitness and distance values will have an impact on the selection of individuals. In this case, the RFDB selection method can be regarded as a symmetrical method. The roulette wheel method is used to determine the high-potential solution candidate, which can be helpful for finding the global optimal solution. The details of the RFDB selection method are explained as follows.

1. Calculate the distance between the i -th osprey and the best osprey.

$$D_{Pi} = \sqrt{(x_{[i,1]} - x_{[best,1]})^2 + (x_{[i,2]} - x_{[best,2]})^2 + \dots + (x_{[i,D]} - x_{[best,D]})^2} \quad (12)$$

2. Form the distance vector.

$$D_P \equiv \begin{bmatrix} d_1 \\ \cdot \\ \cdot \\ \cdot \\ d_m \end{bmatrix} \quad (13)$$

3. Calculate the score of each individual according to the fitness and distance values.

$$S_{Pi} = F \times normf_i + (1 - F) \times normD_{Pi} \quad (14)$$

where F is a weight coefficient set to 0.5. $normf_i$ and $normD_{Pi}$ mean the normalized values of fitness and distance for the i -th individual.

4. Form the RFDB score vector.

$$S_P \equiv \begin{bmatrix} s_1 \\ \cdot \\ \cdot \\ \cdot \\ s_N \end{bmatrix} \quad (15)$$

According to the results of the score vector, the roulette wheel selection method is used to randomly select a candidate individual. Then, refer to Equation (5), and this individual is employed to generate a new position using Equation (16).

$$X_{i,j}^{P2} = X_{i,j} + \frac{X_{RFDB}}{t} \quad (16)$$

where X_{RFDB} is the selected candidate individual using the RFDB selection method from the population.

The flowchart of the proposed MOOA is presented in Figure 2, and the pseudocode is given in Algorithm 2.

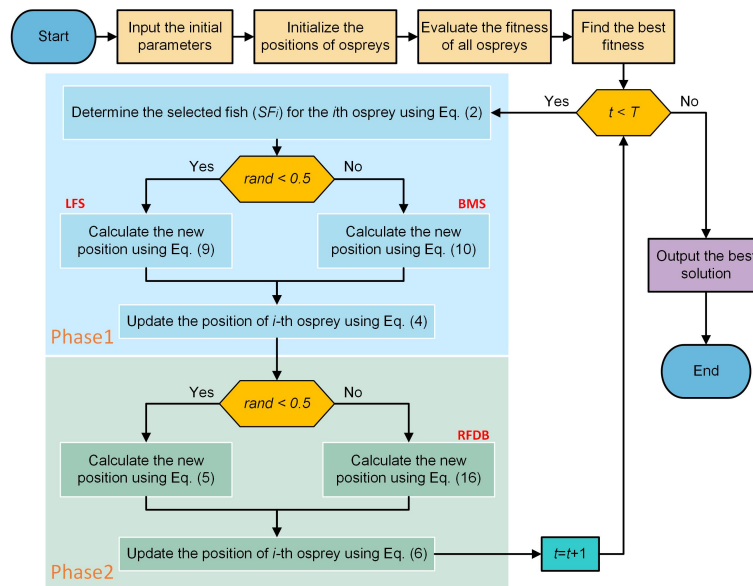


Figure 2. The flowchart of MOOA.

3.3. Time Complexity Analysis of the MOOA

The time complexity is an important indicator for the optimization algorithm [31]. The related influence factors are the initialization, population size N , dimension of optimization problem D , and number of maximum iterations T . In the original OOA, the time complexity of initialization is $O(N \times D)$. The time complexity of phase one is $O(N \times D \times T)$. The time complexity of phase two is $O(N \times D \times T)$. Therefore, the total time complexity of OOA is $O(N \times D \times (2T + 1))$. For the MOOA, the Lévy flight strategy, Brownian motion strategy and fitness–distance balance-based selection method have been applied to improve the basic OOA. In the new phase one and phase two, the time complexity is still $O(N \times D \times T)$. Accordingly, the total time complexity of the MOOA is $O(N \times D \times (2T + 1))$, which is the same as OOA.

Algorithm 2 The pseudocode of the MOOA.

```

1: Input the population size ( $N$ ) and maximum iterations ( $T$ ).
2: Initialize the positions of all ospreys using Equation (1).
3: for  $t = 1$  to  $T$  do
4:   for  $i = 1$  to  $N$  do
5:     Phase 1: Exploring the search space and hunting the fish
6:     Determine the position of fish using Equation (2).
7:     if ( $rand < 0.5$ ) then
8:       Calculate the new position of the osprey using Equation (9).
9:     else
10:      Calculate the new position of the osprey using Equation (10).
11:    end if
12:    Check the boundary conditions and update the  $i$ -th osprey using Equation (4).
13:    Phase 2: Exploiting the search space and carrying the fish
14:    if ( $rand < 0.5$ ) then
15:      Calculate the new position of the osprey using Equation (5).
16:    else
17:      Calculate the new position of the osprey using Equation (16).
18:    end if
19:    Check the boundary conditions and update the  $i$ -th osprey using Equation (6).
20:  end for
21: end for
22: Output the best solution.
  
```

4. Analysis of Experiments and Results

4.1. Experimental Settings

To evaluate the performance of the suggested MOOA, the challenging CEC2017 [32] and CEC2022 [33] benchmark functions are employed. Tables 2 and 3 provide the specific details of these two test suites. More information of CEC2017 and CEC2022 can also be found in other works [34,35].

Table 2. CEC2017 benchmark functions.

Type	No.	Description	F_{min}
Unimodal functions	F1	Shifted and rotated bent cigar function	100
	F3	Shifted and rotated Zakharov function	300
Simple multimodal functions	F4	Shifted and rotated Rosenbrock's function	400
	F5	Shifted and rotated Rastrigin's function	500
	F6	Shifted and rotated expanded scaffer's F6 function	600
	F7	Shifted and rotated Lunacek Bi_Rastrigin function	700
	F8	Shifted and rotated non-continuous Rastrigin's function	800
	F9	Shifted and rotated Lévy function	900
	F10	Shifted and rotated Schwefel's function	1000
	F11	Hybrid function 1 ($N = 3$)	1100
	F12	Hybrid function 2 ($N = 3$)	1200
Hybrid functions.	F13	Hybrid function 3 ($N = 3$)	1300
	F14	Hybrid function 4 ($N = 4$)	1400
	F15	Hybrid function 5 ($N = 4$)	1500
	F16	Hybrid function 6 ($N = 4$)	1600
	F17	Hybrid function 6 ($N = 5$)	1700
	F18	Hybrid function 6 ($N = 5$)	1800
	F19	Hybrid function 6 ($N = 5$)	1900
	F20	Hybrid function 6 ($N = 6$)	2000
	F21	Composition function 1 ($N = 3$)	2100
	F22	Composition function 2 ($N = 3$)	2200
Composition functions	F23	Composition function 3 ($N = 4$)	2300
	F24	Composition function 4 ($N = 4$)	2400
	F25	Composition function 5 ($N = 5$)	2500
	F26	Composition function 6 ($N = 5$)	2600
	F27	Composition function 7 ($N = 6$)	2700
	F28	Composition function 8 ($N = 6$)	2800
	F29	Composition function 9 ($N = 3$)	2900
	F30	Composition function 10 ($N = 3$)	3000

Search range: $[-100, 100]$, Dimension: 10

Table 3. CEC2022 benchmark functions.

Type	No.	Description	F_{min}
Unimodal functions	F1	Shifted and fully rotated Zakharov function	300
	F2	Shifted and fully rotated Rosenbrock's function	400
Simple multimodal functions	F3	Shifted and fully rotated Rastrigin's function	600
	F4	Shifted and fully rotated non-continuous Rastrigin's function	800
	F5	Shifted and fully rotated Lévy function	900
	F6	Hybrid function 1 ($N = 3$)	1800
	F7	Hybrid function 2 ($N = 6$)	2000
Hybrid functions	F8	Hybrid function 3 ($N = 5$)	2200
	F9	Composition function 1 ($N = 5$)	2300
	F10	Composition function 2 ($N = 4$)	2400
	F11	Composition function 3 ($N = 5$)	2600
	F12	Composition function 4 ($N = 6$)	2700

Search range: $[-100, 100]$, Dimension: 10

In addition, the optimization results of the MOOA are compared to eight advanced algorithms, including six standard algorithms as follows: the osprey optimization algorithm (OOA) [25], the Aquila optimization (AO) [36], the arithmetic optimization algorithm (AOA) [10], the chimp optimization algorithm (ChOA) [37], the Harris hawk

optimization (HHO) [38], the grey wolf optimizer (GWO) [9], and two modified algorithms, representative-based grey wolf optimizer (RGWO) [39] and modified particle swarm optimization (MPSO) [40]. The parameter settings of the MOOA and competitive algorithms are given in Table 4. For a fair comparison, the population size and maximum number of iterations of all methods are set to 30 and 500, respectively. Each test function is independently performed 30 times to eliminate the effect of randomness.

Table 4. Parameter settings for optimization algorithms.

Algorithm	Year	Parameters
MOOA	-	$r_1 \in [0, 1]$, $P=0.5$, $CF = (1 - t/T)^{2 \times t/T}$
OOA	2023	$r_1 \in [0, 1]$
AO	2021	$\alpha = 0.1$, $\delta = 0.1$
AOA	2021	$\alpha = 5$, $\mu = 0.499$
ChOA	2020	Control parameter $f \in [0, 2]$
HHO	2019	Initial Energy $E_0 \in [-1, 1]$
GWO	2014	Convergence parameter $a = 2 \times (1 - t/T)$
RGWO	2021	$\sigma_{initial} = 1$, $\sigma_{final} = 0$, Exponent = 2
MPSO	2009	Cognitive coefficient $c_1 = 2.55 - 2.05 \times t/T$, Social coefficient $c_2 = 1.25 + t/T$, Inertia weight W linearly decreased in $[0.9, 0.4]$

4.2. Experimental Series 1: CEC2017 Benchmark Functions

Table 5 provides the mean, best, worst, Std and Friedman ranking results of the MOOA and other comparison algorithms on the CEC2017 functions [41]. The best mean values among these algorithms are marked in bold. By observing the results, it is found that the MOOA obtains the lowest mean values on 19 test functions, including F1, F4, F5, F8, F10, F12, F13, F16-F19, F21-F27, and F30, indicating the MOOA's superior performance in solving CEC2017 problems compared to other methods. For other benchmark functions, the MOOA also obtains good optimal values except for F3, F6, F7, and F9. On the whole, the MOOA outperforms the basic OOA and other algorithms, demonstrating the outstanding search capability of the MOOA. In addition, according to the mean ranking results given in Table 5, the MOOA obtains the smallest average rank of 1.66 and ranks first, followed by the RGWO, MPSO, GWO, AO, HHO, ChOA, AOA, and OOA. Therefore, the global and local search performance of basic OOA is substantially enhanced by applying effective improvement strategies, including the Lévy flight strategy, the Brownian motion strategy and the RFDB selection method.

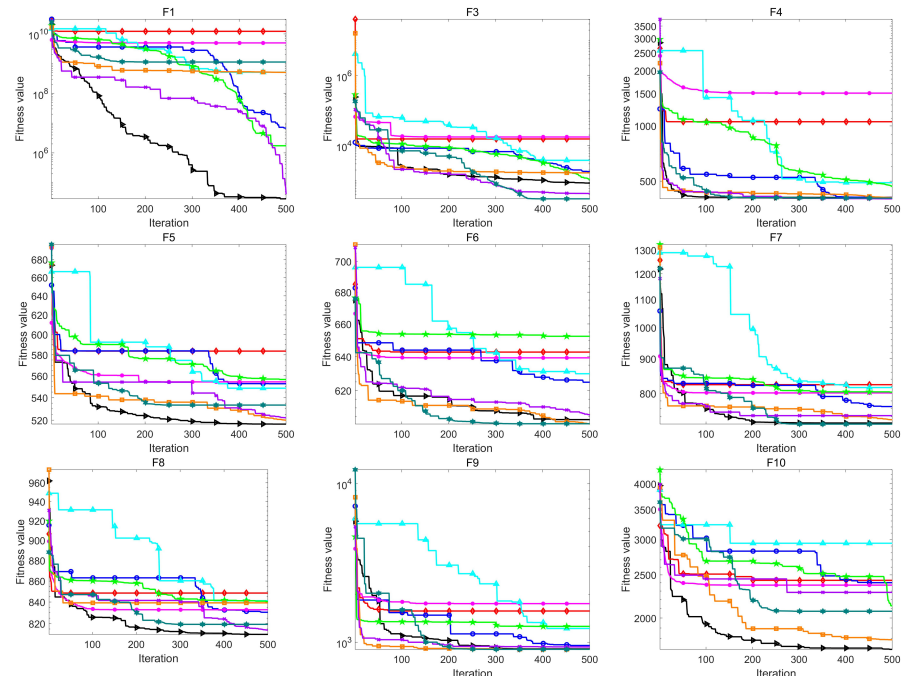
Table 5. Numerical results of the MOOA and other comparison algorithms on CEC2017.

Function	Index	MOOA	OOA	AO	AOA	ChOA	HHO	GWO	RGWO	MPSO
F1	Mean	4.395E+05	9.913E+09	2.604E+07	7.909E+09	2.250E+09	1.590E+06	2.383E+07	1.363E+07	4.079E+08
	Best	8.625E+04	3.718E+09	9.494E+05	1.730E+09	4.204E+08	1.967E+05	2.427E+04	4.898E+04	1.321E+03
	Worst	4.477E+06	2.274E+10	1.760E+08	1.645E+10	4.692E+09	7.429E+06	3.721E+08	3.427E+08	1.807E+09
	Std	7.917E+05	4.835E+09	3.929E+07	3.667E+09	1.701E+09	1.703E+06	8.124E+07	6.248E+07	6.142E+08
	Rank	1	9	5	8	7	2	4	3	6
F3	Mean	2.553E+03	1.305E+04	2.419E+03	1.264E+04	4.702E+03	7.649E+02	3.374E+03	7.481E+02	5.709E+02
	Best	1.125E+03	6.009E+03	4.706E+02	5.373E+03	1.998E+03	3.162E+02	3.168E+02	3.045E+02	3.000E+02
	Worst	4.188E+03	1.996E+04	3.925E+03	1.754E+04	8.540E+03	1.842E+03	1.057E+04	2.784E+03	4.554E+03
	Std	8.693E+02	3.862E+03	8.808E+02	3.207E+03	1.910E+03	4.143E+02	2.673E+03	7.698E+02	9.251E+02
	Rank	5	9	4	8	7	3	6	2	1
F4	Mean	4.092E+02	1.144E+03	4.266E+02	1.143E+03	6.133E+02	4.366E+02	4.167E+02	4.188E+02	4.274E+02
	Best	4.017E+02	5.695E+02	4.052E+02	5.247E+02	4.566E+02	4.004E+02	4.004E+02	4.035E+02	4.042E+02
	Worst	4.385E+02	3.558E+03	5.088E+02	2.224E+03	8.835E+02	5.657E+02	4.949E+02	4.801E+02	5.156E+02
	Std	7.374E+00	5.646E+02	2.646E+01	4.483E+02	1.348E+02	4.639E+01	1.935E+01	2.145E+01	3.154E+01
	Rank	1	9	4	8	7	6	2	3	5
F5	Mean	5.153E+02	5.849E+02	5.350E+02	5.638E+02	5.624E+02	5.622E+02	5.174E+02	5.155E+02	5.259E+02
	Best	5.065E+02	5.425E+02	5.200E+02	5.353E+02	5.388E+02	5.301E+02	5.060E+02	5.030E+02	5.080E+02
	Worst	5.225E+02	6.129E+02	5.625E+02	6.244E+02	5.982E+02	6.006E+02	5.298E+02	5.433E+02	5.543E+02
	Std	3.886E+00	1.916E+01	9.916E+00	1.816E+01	1.171E+01	2.102E+01	6.959E+00	9.126E+00	9.973E+00
	Rank	1	9	5	8	7	6	3	2	4

Table 7. Cont.

Function	MOOA	OOA	AO	AOA	ChOA	HHO	GWO	RGWO	MPSO
F16	1.920E-01	1.071E-01	1.369E-01	5.419E-02	4.357E-01	1.395E-01	5.256E-02	1.339E-01	5.223E-02
F17	2.199E-01	1.312E-01	1.664E-01	6.939E-02	4.579E-01	1.740E-01	6.567E-02	1.754E-01	6.610E-02
F18	1.949E-01	1.065E-01	1.392E-01	5.574E-02	4.431E-01	1.467E-01	5.300E-02	1.361E-01	5.228E-02
F19	3.565E-01	2.692E-01	3.015E-01	1.357E-01	5.293E-01	3.430E-01	1.326E-01	3.777E-01	1.350E-01
F20	2.221E-01	1.309E-01	1.648E-01	6.833E-02	4.664E-01	1.794E-01	6.654E-02	1.778E-01	6.906E-02
F21	2.307E-01	1.393E-01	1.774E-01	7.247E-02	4.653E-01	1.796E-01	6.972E-02	1.882E-01	6.903E-02
F22	2.436E-01	1.555E-01	1.887E-01	8.012E-02	4.662E-01	2.001E-01	7.935E-02	2.134E-01	7.910E-02
F23	2.496E-01	1.603E-01	1.957E-01	8.404E-02	4.791E-01	2.109E-01	8.202E-02	2.218E-01	8.092E-02
F24	2.684E-01	1.738E-01	2.101E-01	9.064E-02	4.858E-01	2.218E-01	8.609E-02	2.384E-01	8.611E-02
F25	2.405E-01	1.502E-01	1.832E-01	7.896E-02	4.662E-01	1.894E-01	7.474E-02	2.041E-01	7.463E-02
F26	2.718E-01	1.826E-01	2.185E-01	9.679E-02	4.937E-01	2.321E-01	9.077E-02	2.525E-01	9.000E-02
F27	2.871E-01	1.942E-01	2.269E-01	1.000E-01	5.021E-01	2.396E-01	9.724E-02	2.652E-01	9.471E-02
F28	2.613E-01	1.713E-01	2.076E-01	8.917E-02	4.781E-01	1.914E-01	8.507E-02	2.336E-01	8.472E-02
F29	2.591E-01	1.662E-01	2.051E-01	8.750E-02	4.793E-01	2.214E-01	8.626E-02	2.285E-01	8.489E-02
F30	3.912E-01	3.034E-01	3.367E-01	1.518E-01	5.422E-01	3.686E-01	1.474E-01	4.227E-01	1.521E-01

The convergence curves of all algorithms on the CEC2017 test set are shown in Figures 3 and 4. It is observed that the MOOA has the ability to find newer optimal values, while other algorithms display the problem of stagnation. In the early stage, the MOOA shows remarkable exploration ability compared to other algorithms on F1, F5, F10, F12, F13, F15, F19, F21, F24, F28, and F30. Meanwhile, the MOOA also presents sufficient optimization accuracy on F1, F10, F12, F16, F21, F24, and F29 in the later stage. Thus, the convergence analysis confirms the optimizing capabilities of the MOOA during the iterations.

**Figure 3.** Cont.

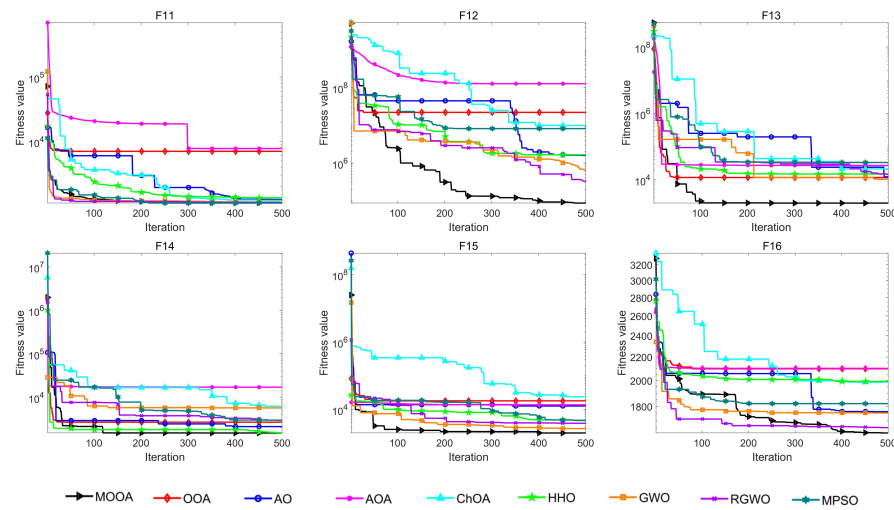


Figure 3. Convergence curves of the MOOA and other algorithms on CEC2017 (F1, F3–F16).

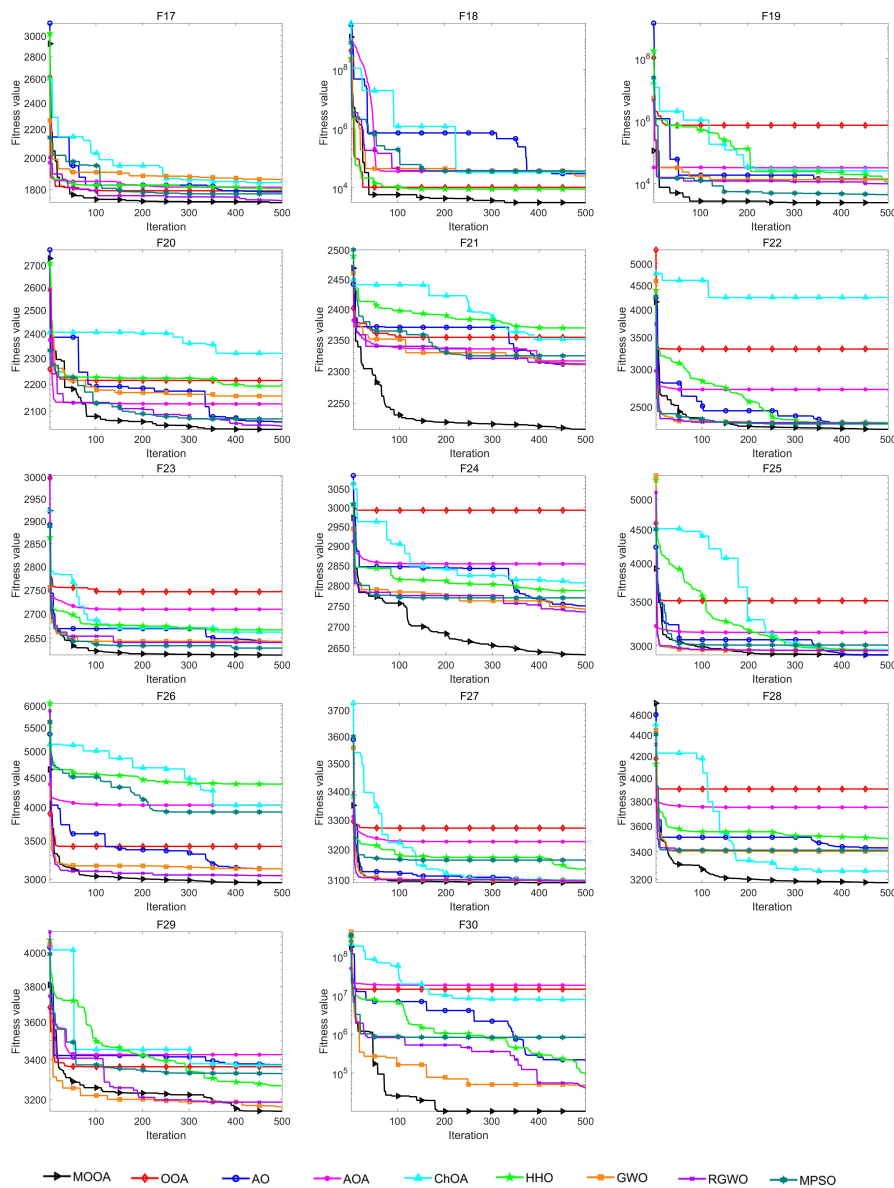


Figure 4. Convergence curves of the MOOA and other algorithms on CEC2017 (F17–F30).

Figures 5 and 6 show the box diagrams of the MOOA and competing algorithms on CEC2017 test functions. It is evident that the MOOA has the narrowest box plots on the majority of functions, such as F4, F5, F7, F8, F10, F11, F13–F20, F22–F27, and F29, indicating that the MOOA has stable and robust performance on these functions. Moreover, the MOOA also achieves lower positions on most of the functions, such as F4, F13, F16–F19, F21, F23, and F27, suggesting that the MOOA has the ability to obtain an optimal solution with higher precision. In addition, the MOOA shows fewer outliers (+) on most of the test functions, which means the MOOA is more stable when solving these problems.

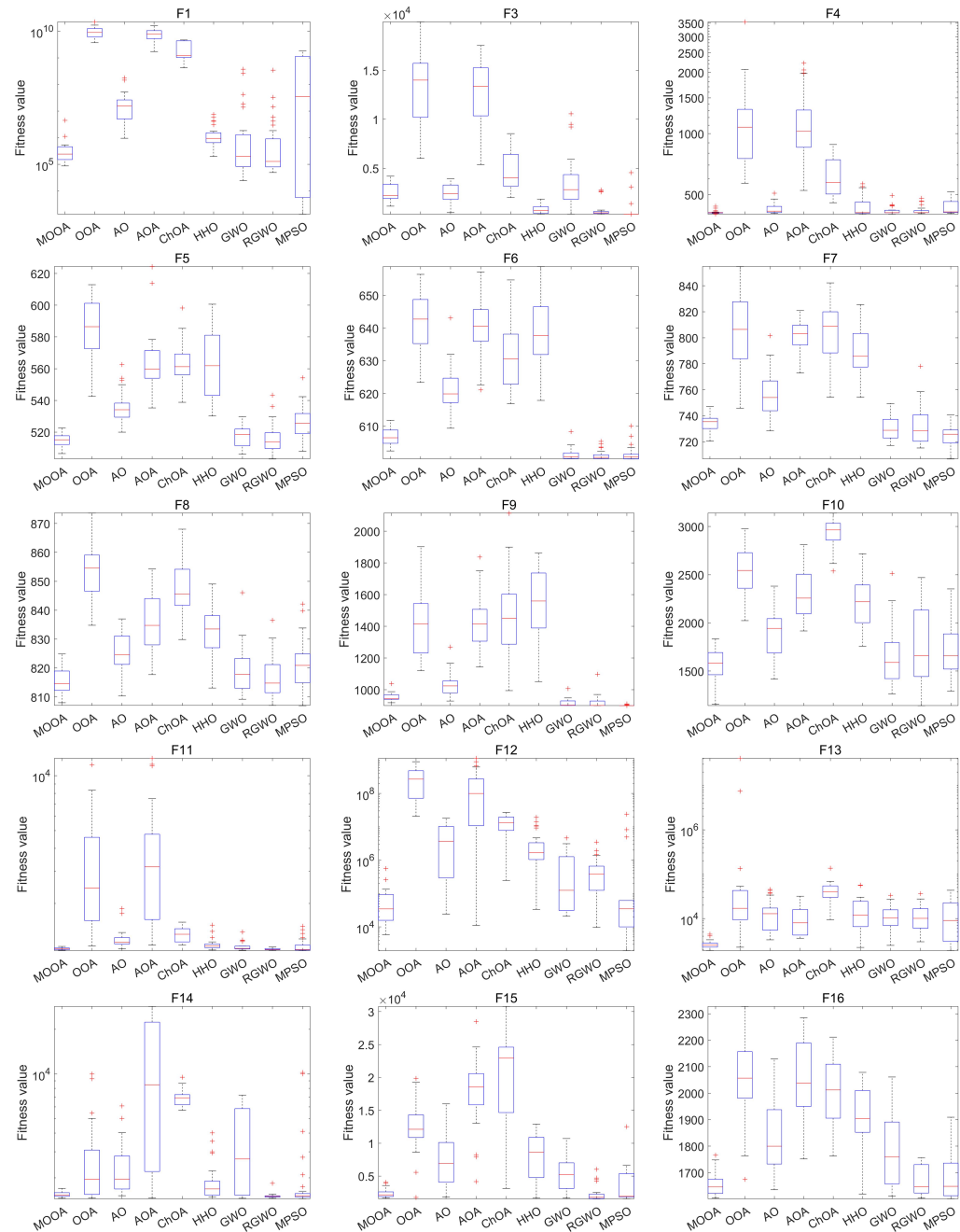


Figure 5. Boxplots of the MOOA and other algorithms on CEC2017 (F1, F3–F16).

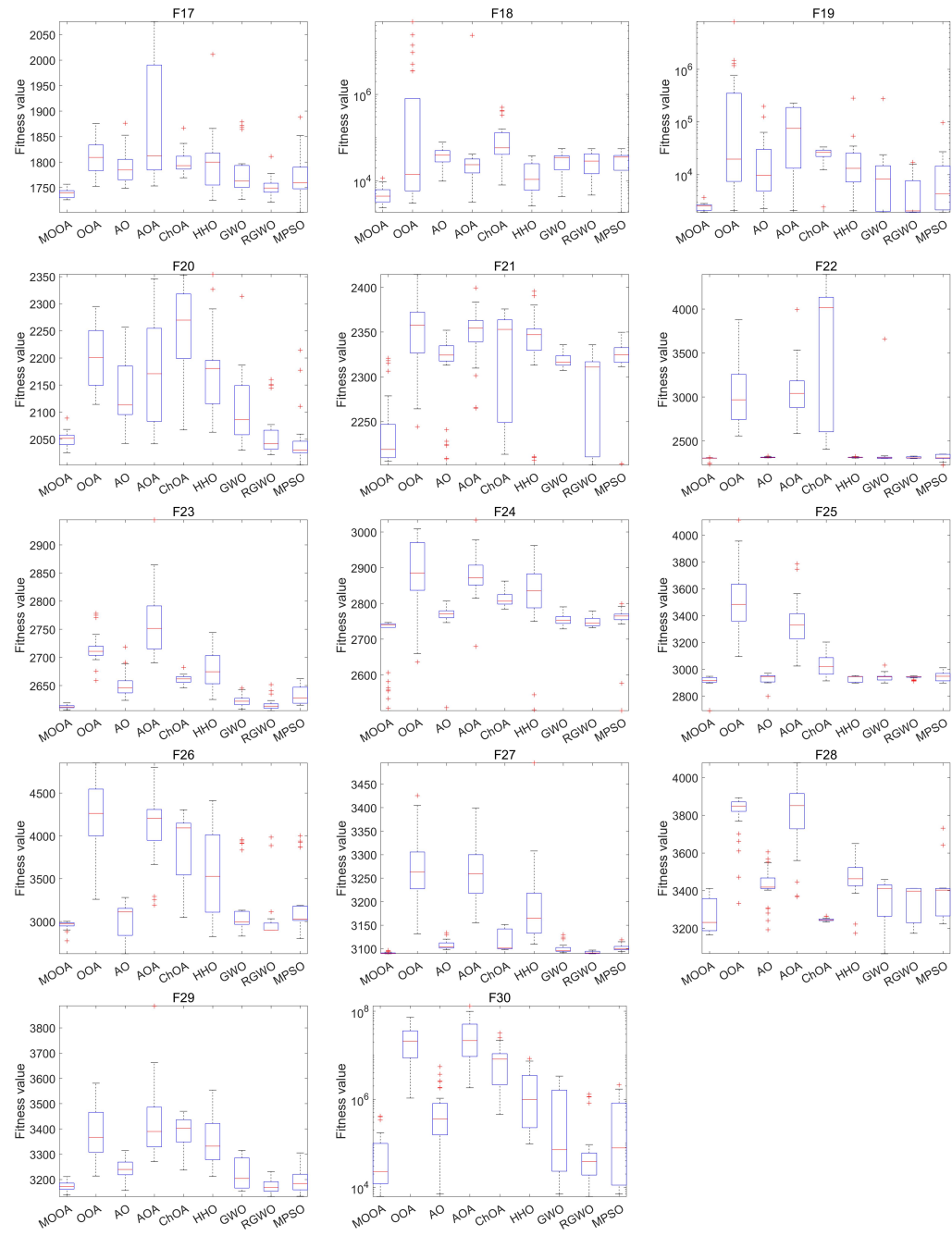


Figure 6. Boxplots of the MOOA and other algorithms on CEC2017 (F17–F30).

Figure 7 shows the ranking radar maps of the MOOA and other compared algorithms. It is evident that the shaded area of the MOOA is the smallest, and RGWO follows it. And the OOA, AOA and ChOA display a larger shaded area. In fact, according to Table 5, the MOOA ranks first on most of the test functions. Therefore, the MOOA has better performance in solving CEC2017 problems compared to other methods.

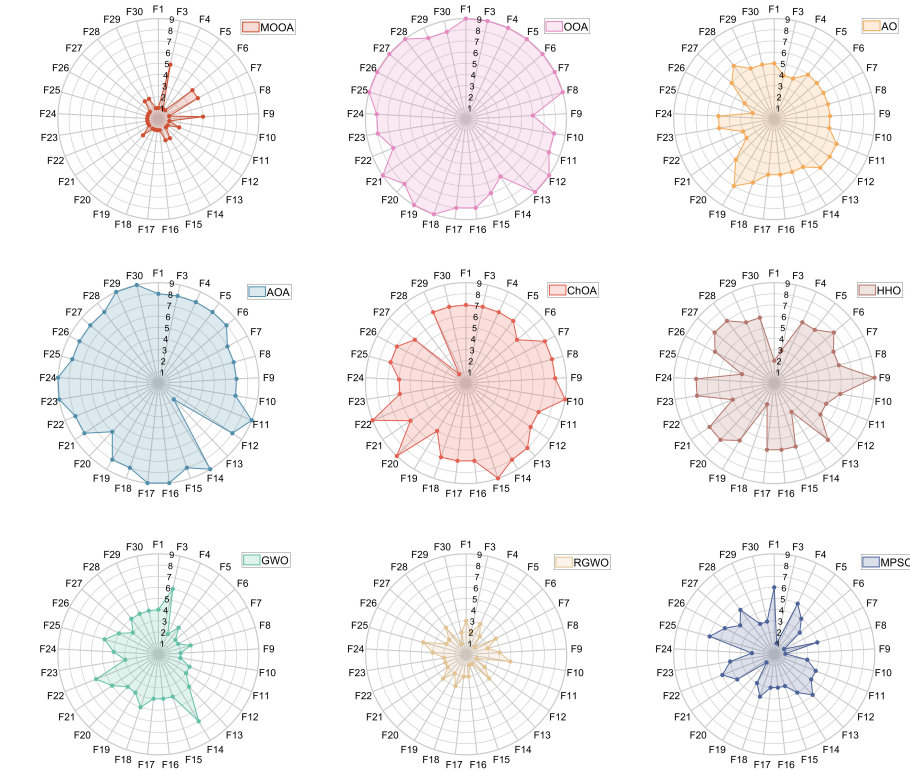


Figure 7. Radar plots of the MOOA and other algorithms on CEC2017.

4.3. Experimental Series 2: CEC2022 Benchmark Functions

The statistical results of all algorithms on the CEC2022 functions are provided in Table 8. The MOOA obtains the best mean values in 8 of 12 test functions, which are F2, F4, F6, and F8-F12. However, the MOOA did not achieve good performance in F1 and only ranked seventh. Nevertheless, compared to the basic OOA, the MOOA shows obvious improvements in all test functions. According to the results of the Friedman ranking test, the MOOA ranks first with a mean rank value of 2.17, suggesting the MOOA's superior performance on CEC2022.

Table 8. Numerical results of the MOOA and other comparison algorithms on CEC2022.

Function	Index	MOOA	OOA	AO	AOA	ChOA	HHO	GWO	RGWO	MPSO
F1	Mean	6.826E+03	8.624E+03	4.388E+03	1.251E+04	5.364E+03	1.133E+03	3.077E+03	6.476E+02	4.805E+02
	Best	1.748E+03	3.858E+03	6.956E+02	6.645E+03	2.473E+03	4.044E+02	3.975E+02	3.048E+02	3.000E+02
	Worst	1.190E+04	1.163E+04	1.161E+04	2.520E+04	1.100E+04	2.569E+03	9.171E+03	4.312E+03	3.236E+03
	Std	2.351E+03	1.953E+03	2.278E+03	4.353E+03	1.763E+03	5.671E+02	2.276E+03	7.656E+02	6.756E+02
	Rank	7	8	5	9	6	3	4	2	1
F2	Mean	4.077E+02	1.573E+03	4.695E+02	1.621E+03	6.587E+02	4.454E+02	4.231E+02	4.238E+02	4.589E+02
	Best	4.016E+02	6.778E+02	4.095E+02	5.369E+02	4.624E+02	4.005E+02	4.002E+02	4.005E+02	4.079E+02
	Worst	4.094E+02	2.902E+03	6.876E+02	5.189E+03	1.128E+03	5.933E+02	4.713E+02	4.734E+02	8.159E+02
	Std	2.178E+00	5.835E+02	6.675E+01	9.755E+02	1.727E+02	4.492E+01	2.165E+01	2.507E+01	9.458E+01
	Rank	1	8	6	9	7	4	2	3	5
F3	Mean	6.068E+02	6.418E+02	6.212E+02	6.406E+02	6.319E+02	6.408E+02	6.014E+02	6.019E+02	6.018E+02
	Best	6.036E+02	6.238E+02	6.057E+02	6.246E+02	6.156E+02	6.206E+02	6.001E+02	6.001E+02	6.000E+02
	Worst	6.135E+02	6.578E+02	6.400E+02	6.521E+02	6.699E+02	6.620E+02	6.060E+02	6.092E+02	6.051E+02
	Std	2.448E+00	9.478E+00	7.997E+00	7.013E+00	1.137E+01	1.056E+01	1.558E+00	2.372E+00	1.630E+00
	Rank	4	9	5	7	6	8	1	3	2
F4	Mean	8.128E+02	8.477E+02	8.241E+02	8.389E+02	8.431E+02	8.273E+02	8.189E+02	8.181E+02	8.215E+02
	Best	8.031E+02	8.231E+02	8.120E+02	8.219E+02	8.251E+02	8.120E+02	8.060E+02	8.061E+02	8.070E+02
	Worst	8.205E+02	8.662E+02	8.363E+02	8.632E+02	8.560E+02	8.409E+02	8.560E+02	8.418E+02	8.447E+02
	Std	3.782E+00	1.021E+01	5.862E+00	9.129E+00	7.897E+00	7.730E+00	1.175E+01	8.262E+00	9.560E+00
	Rank	1	9	5	7	8	6	3	2	4
F5	Mean	9.434E+02	1.382E+03	1.079E+03	1.352E+03	1.288E+03	1.425E+03	9.231E+02	9.174E+02	9.020E+02
	Best	9.066E+02	1.091E+03	9.533E+02	1.108E+03	1.057E+03	1.114E+03	9.001E+02	9.000E+02	9.000E+02
	Worst	9.942E+02	1.931E+03	1.374E+03	1.833E+03	1.795E+03	1.904E+03	1.028E+03	1.051E+03	9.063E+02
	Std	2.195E+01	1.930E+02	8.643E+01	1.675E+02	2.002E+02	1.945E+02	3.134E+01	3.185E+01	2.105E+00
	Rank	4	8	5	7	6	9	3	2	1

Table 10. Comparison results of average running time (seconds) over 30 independent runs on CEC2022.

Function	MOOA	OOA	AO	AOA	ChOA	HHO	GWO	RGWO	MPSO
F1	1.612E-01	7.441E-02	1.018E-01	4.434E-02	4.295E-01	9.798E-02	3.899E-02	8.892E-02	3.795E-02
F2	1.515E-01	6.800E-02	9.653E-02	4.119E-02	4.189E-01	8.813E-02	3.681E-02	8.448E-02	3.472E-02
F3	1.870E-01	1.059E-01	1.340E-01	5.959E-02	4.378E-01	1.406E-01	5.684E-02	1.438E-01	5.347E-02
F4	1.589E-01	7.933E-02	1.092E-01	4.776E-02	4.197E-01	1.098E-01	4.248E-02	1.035E-01	4.101E-02
F5	1.691E-01	8.775E-02	1.161E-01	5.051E-02	4.213E-01	1.190E-01	4.598E-02	1.112E-01	4.395E-02
F6	1.568E-01	7.332E-02	1.018E-01	4.318E-02	4.168E-01	1.008E-01	3.853E-02	8.897E-02	3.769E-02
F7	2.152E-01	1.267E-01	1.561E-01	7.078E-02	4.511E-01	1.684E-01	6.633E-02	1.734E-01	7.116E-02
F8	2.389E-01	1.496E-01	1.800E-01	8.293E-02	4.663E-01	1.970E-01	7.774E-02	2.084E-01	7.821E-02
F9	2.049E-01	1.178E-01	1.520E-01	6.772E-02	4.498E-01	1.526E-01	6.322E-02	1.625E-01	6.152E-02
F10	1.972E-01	1.114E-01	1.431E-01	6.340E-02	4.441E-01	1.460E-01	5.819E-02	1.486E-01	5.634E-02
F11	2.345E-01	1.467E-01	1.776E-01	8.355E-02	4.726E-01	1.849E-01	7.670E-02	2.022E-01	7.440E-02
F12	2.418E-01	1.531E-01	1.851E-01	8.592E-02	4.697E-01	1.976E-01	7.895E-02	2.149E-01	7.781E-02

Figure 8 presents the convergence curves of all algorithms on the CEC2022 test set. It is noted that the MOOA has a faster convergence speed than other algorithms on all functions except for F1 and F3. For the unimodal function F1 and simple multimodal function F3, the MOOA still performs better than the OOA. Hence, the proposed MOOA has good convergence speed and accuracy in solving the problems of CEC2022.

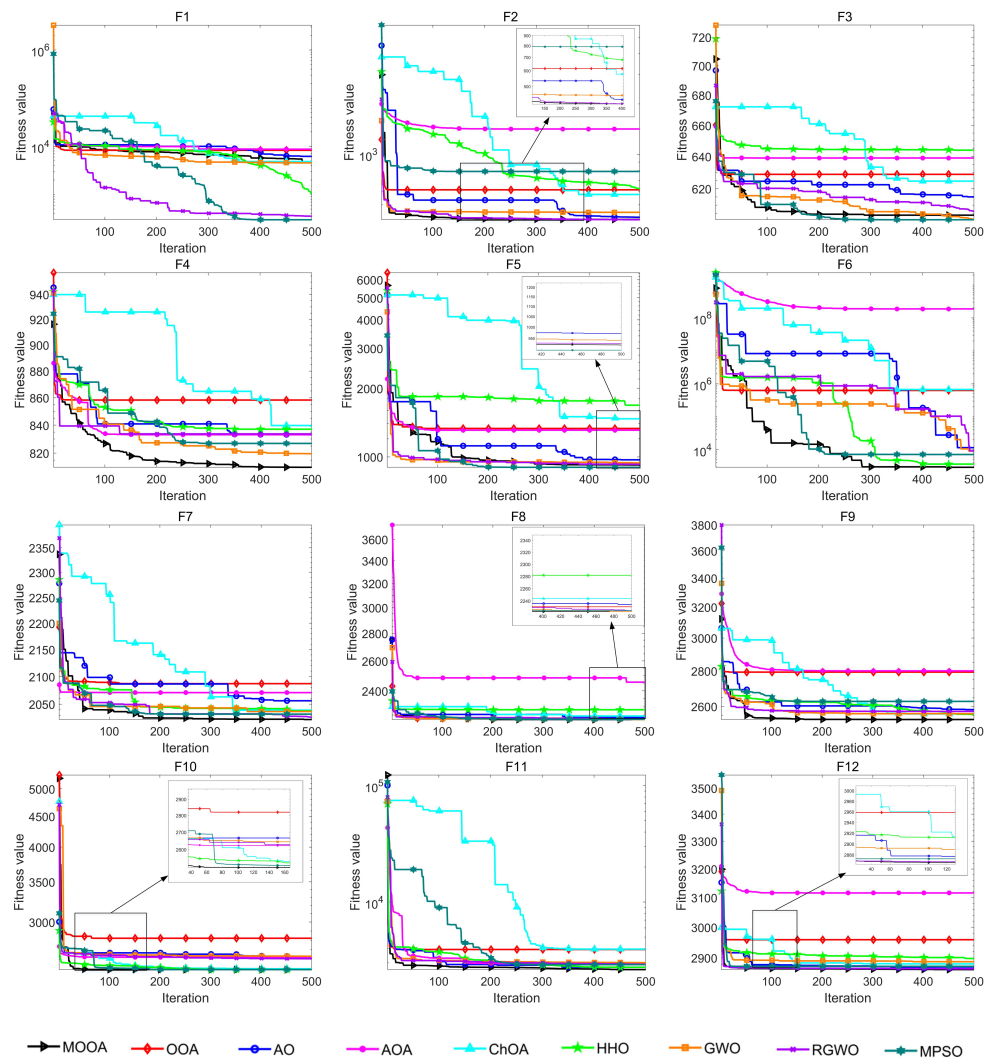


Figure 8. Convergence curves of the MOOA and other algorithms on CEC2022.

Figure 9 shows the boxplots of the MOOA and other algorithms on CEC2022 test functions. It is observed that the MOOA shows the narrowest and lowest box plots on functions F2, F4, F6, F8, F9, F10, and F12, indicating that it has good algorithm stability in solving these problems. The MOOA also displays comparable results on other functions. This further confirms the superior performance of the MOOA on CEC2022.

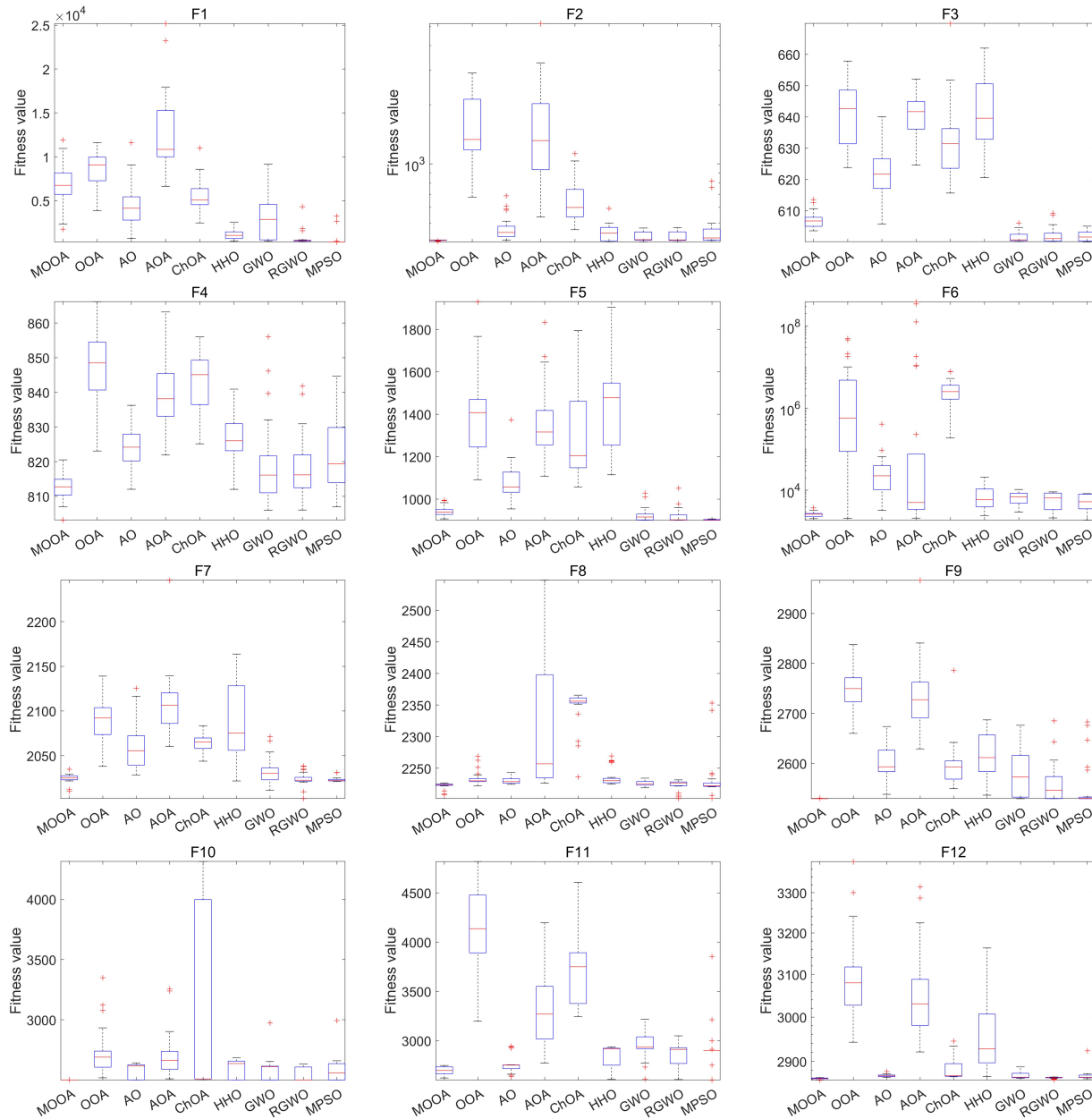


Figure 9. Boxplots of the MOOA and other algorithms on CEC2022.

Figure 10 displays the ranking radar maps of the MOOA and other compared algorithms on CEC2022. It is shown that the MOOA has better or comparable ranking results than other compared methods on all test functions except for the F1. Compared to the original OOA, the proposed method exhibits excellent performance on CEC2022 functions, indicating the efficacy of the applied improvements.

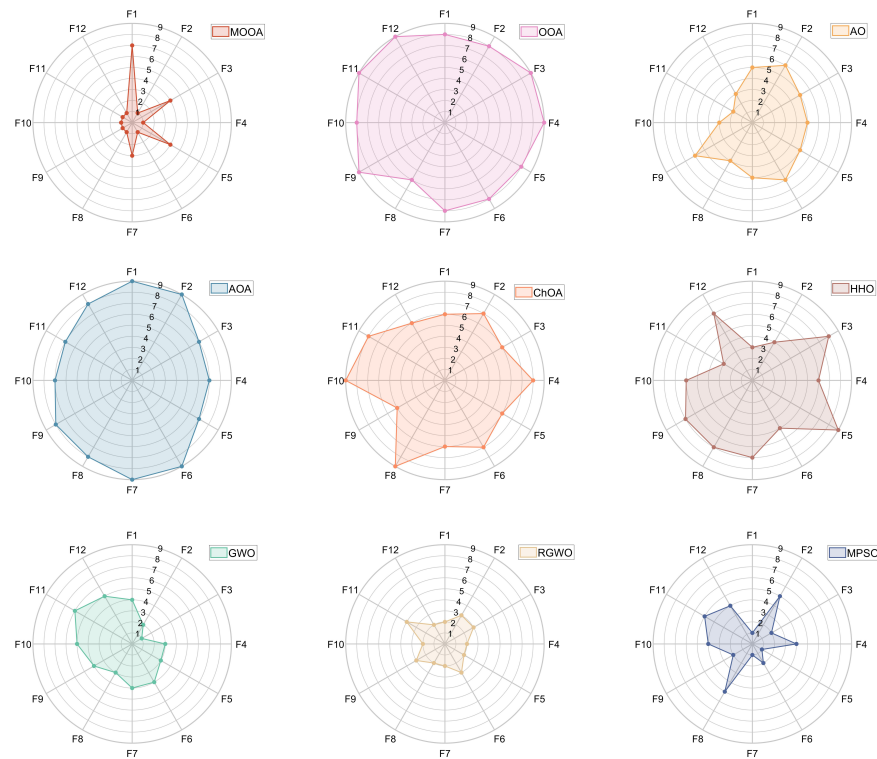


Figure 10. Radar plots of the MOOA and other algorithms on CEC2022.

5. Applicability of the MOOA for Solving Engineering Problems

In this section, the MOOA's ability in handling practical engineering applications is tested using five engineering optimization problems, including the welded beam design problem, the three-bar truss design problem, the tension/compression spring design problem, the pressure vessel design problem, and the tubular column design problem. In these engineering design optimization problems, variables need to be optimized with the given multiple inequality constraints [43]. The experimental conditions and comparison algorithms are consistent with the previous experiments.

5.1. Welded Beam Design Problem

The objective of the welded beam design problem is to optimize four variables with seven constraints to reduce the cost of fabricating [44], as shown in Figure 11. These decision variables include the welding thickness (h), rod attachment length (l), rod height (t), and rod thickness (b). The mathematical model of this issue can be expressed in Equation (17).

Table 11 displays the optimal results of the MOOA and other algorithms. The results indicate that the MOOA provides the best solution in dealing with this issue. The lowest cost obtained by the MOOA is 1.702268716, and the corresponding design variables are [0.204451219, 3.277077923, 9.034062643, 0.206541308].

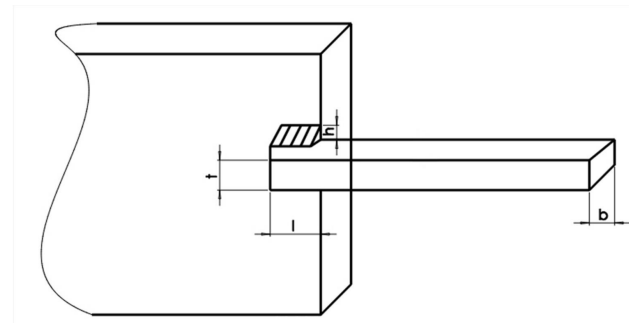


Figure 11. Structural parameters of the welded beam design problem.

Consider variable $\vec{z} = [z_1, z_2, z_3, z_4] = [h, l, t, b]$.

Minimize $f(\vec{z}) = 1.10471z_1^2z_2 + 0.04811z_3z_4(14 + z_2)$.

Subject to $g_1(\vec{z}) = \tau(z) - \tau_{\max} \leq 0$,
 $g_2(\vec{z}) = \sigma(z) - \sigma_{\max} \leq 0$,
 $g_3(\vec{z}) = z_1 - z_4 \leq 0$,
 $g_4(\vec{z}) = 0.10471z_1^2 + 0.04811z_3z_4(14 + z_2) - 5 \leq 0$,
 $g_5(\vec{z}) = 0.125 - z_1 \leq 0$,
 $g_6(\vec{z}) = \delta(z) - \delta_{\max} \leq 0$,
 $g_7(\vec{z}) = P - P_c(z) \leq 0$.

Variable range $0.1 \leq z_1, z_4 \leq 2$,
 $0.1 \leq z_2, z_3 \leq 10$.

where $\tau(z) = \sqrt{(\tau')^2 + 2\tau'\tau'' \frac{z_2}{2R} + (\tau'')^2}$,
 $\tau' = \frac{P}{\sqrt{2z_1z_2}}, \quad \tau'' = \frac{MR}{J}$,
 $M = P\left(L + \frac{z_2}{2}\right)$,
 $R = \sqrt{\frac{z_2^2}{4} + \left(\frac{z_1 + z_3}{2}\right)^2}$,
 $J = 2\left\{\sqrt{2}z_1z_2\left[\frac{z_2^2}{12} + \left(\frac{z_1 + z_3}{2}\right)^2\right]\right\}$,
 $\sigma(z) = \frac{6PL}{z_4\chi_3^2}, \quad \delta(z) = \frac{4PL^3}{Ez_3^3z_4}$,
 $P_c(z) = \frac{4.013E\sqrt{\frac{z^2z^5}{36}}}{L^2}\left(1 - \frac{z_3}{2L}\sqrt{\frac{E}{4G}}\right)$.

$P = 6000 \text{ lb}$, $L = 14 \text{ in}$, $E = 30 \times 10^6 \text{ psi}$, $G = 12 \times 10^6 \text{ psi}$,
 $\tau_{\max} = 13,600 \text{ ps}$, $\sigma_{\max} = 30,000 \text{ psi}$, $\delta_{\max} = 0.25 \text{ in}$.

Table 11. Comparison of optimization results for welded beam design problem.

Algorithm	Optimal Values for Variables				Optimal Cost
	<i>h</i>	<i>l</i>	<i>t</i>	<i>b</i>	
MOOA	0.204451219	3.277077923	9.034062643	0.206541308	1.702268716
OOA	0.125211615	6.968881248	8.906767944	0.214356155	2.046744398
AO	0.16846836	4.473191471	8.825467151	0.22420134	1.898793692
AOA	0.193723284	3.665171957	10	0.205982882	1.902541601
ChOA	0.18225704	3.626627825	9.476918306	0.205193925	1.7821413
HHO	0.177337115	3.759610923	9.541952824	0.203338557	1.788390057
GWO	0.197813447	3.403387574	9.032696795	0.206102119	1.705843204
RGWO	0.20056831	3.364777682	9.038637479	0.205775649	1.703353286
MPSO	0.201386666	3.087096048	10	0.201380645	1.793785741

5.2. Pressure Vessel Design Problem

The pressure vessel design problem aims at minimizing the cost of raw materials for a pressure vessel [45]. As shown in Figure 12, four structural parameters are required to be optimized, including the thickness of shell (T_s), thickness of head (T_h), inner radius (R), and length of headless cylindrical section (L). The mathematical formulas are described in Equation (18).

Table 12 gives the optimal results of the MOOA. It is observed that the MOOA has the lowest cost with 5735.548303, and GWO follows it. And the optimal variables [T_s, T_h, R, L] obtained by the

MOOA are [0.740087552, 0.370680718, 40.31983229, 199.999164]. Therefore, the proposed algorithm has the superiority in solving this design problem.

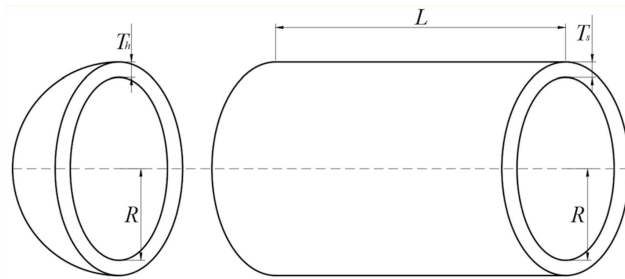


Figure 12. Structural parameters of the pressure vessel problem.

$$\begin{aligned}
 & \text{Consider variable } \vec{y} = [y_1, y_2, y_3, y_4] = [T_s, T_h, R, L]. \\
 & \text{Minimize} \quad f(\vec{y}) = 0.6224y_1y_3y_4 + 1.7781y_2y_3^2 + \\
 & \quad 3.1661y_1^2y_4 + 19.84y_1^2y_3. \\
 & \text{Subject to} \quad g_1(\vec{y}) = -y_1 + 0.0193y. \\
 & \quad g_2(\vec{y}) = -y_2 + 0.00954y_3 \leq 0. \\
 & \quad g_3(\vec{y}) = -\pi y_3^2y_4 - 4/3\pi y_3^3 + 1296,000 \leq 0. \\
 & \quad g_4(\vec{y}) = y_4 - 240 \leq 0. \\
 & \text{Variable range} \quad 0 \leq y_1, y_2 \leq 99. \\
 & \quad 10 \leq y_3, y_4 \leq 200.
 \end{aligned} \tag{18}$$

Table 12. Comparison of optimization results for the pressure vessel design problem.

Algorithm	Optimal Values for Variables				Optimal Cost
	<i>h</i>	<i>l</i>	<i>t</i>	<i>b</i>	
MOOA	0.740087552	0.370680718	40.31983229	199.999164	5735.548303
OOA	4.792398789	4.017954008	60.42998669	32.44395666	61832.69084
AO	0.842322333	0.379594948	44.87225728	145.0998081	6021.401007
AOA	0.022655643	1.029523791	41.01793224	200	62330.97627
ChOA	0	0.427474984	40.33158559	200	61826.98971
HHO	0.945927184	0.466339982	50.73848623	92.77408339	6211.997644
GWO	0.740927138	0.366485948	40.32884403	199.9022614	5737.618222
RGWO	0.744027303	0.366888522	40.42888035	198.5316579	5741.931252
MPSO	0.90382049	0.440300815	48.31912462	112.2665527	6078.183974

5.3. Tubular Column Design Problem

The objective of the tubular column design problem is to minimize the cost while withstanding the compression loads of P [46]. Figure 13 illustrates the structure of a uniform tubular column and its cross-section. Two variables need to be determined: the average column diameter (d) and the tube thickness (t). In this issue, the length of column l is 250 cm. The modulus of elasticity E is 0.85106 kgf/cm², and the yield stress σ_y is 500 kgf/cm². The mathematical model of this problem is given in Equation (19).

As shown in Table 13, the MOOA has obtained the lowest cost, which is 26.53261381. The corresponding variables are 5.451801164, 0.291930864, respectively. Thus, the MOOA shows good performance in solving this problem compared to other methods.

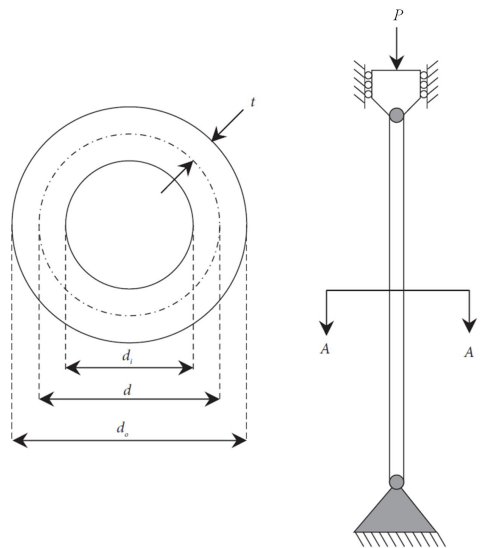


Figure 13. Structural parameters of the tubular column design problem.

$$\begin{aligned}
 & \text{Minimize} && f(d, t) = 9.8dt + 2d \\
 & \text{Subject to} && g_1 = \frac{P}{\pi dt \sigma_y} - 1 \leq 0 \\
 & && g_2 = \frac{9PL^2}{\pi^3 E dt (d^2 + t^2)} - 1 \leq 0 \\
 & && g_3 = \frac{2.0}{d} - 1 \leq 0 \\
 & && g_4 = \frac{d}{14} - 1 \leq 0 \\
 & && g_5 = \frac{0.2}{t} - 1 \leq 0 \\
 & && g_6 = \frac{t}{0.8} - 1 \leq 0 \\
 & \text{Variable range} && 0.01 \leq d, t \leq 100
 \end{aligned} \tag{19}$$

Table 13. Comparison of optimization results for the tubular column design problem.

Algorithm	Optimal Values for Variables		Optimal Cost
	d	t	
MOOA	5.451801164	0.291930864	26.53261381
OOA	5.605087619	0.284065515	26.84569808
AO	5.542489228	0.288159103	26.76868431
AOA	5.723901675	0.278064003	27.07742347
ChOA	5.431743862	0.296824343	26.69601648
HHO	5.429447697	0.29545272	26.61163051
GWO	5.452810323	0.291862615	26.53626955
RGWO	5.450408776	0.292253423	26.54310167
MPSO	5.470173495	0.29084307	26.6998997

5.4. Three-Bar Truss Design Problem

The goal of the three-bar truss design problem is to obtain the minimum weight of the three-bar truss structure [47]. As shown in Figure 14, two variables are required to be optimized: the cross-sectional regions A_1 and A_2 . The formulas are described in Equation (20).

Table 14 provides the optimal results obtained by the MOOA and other compared approaches. It is shown that the MOOA outperforms other algorithms with a minimum weight of 263.8523476, whereas MPSO follows it with a close result of 263.8523691.

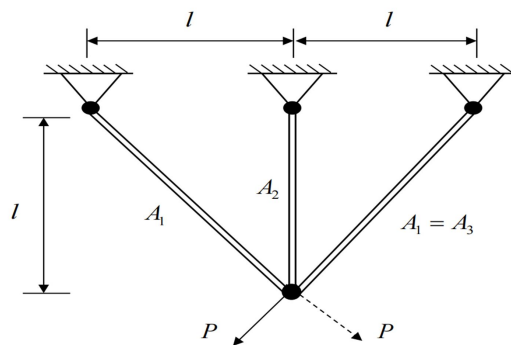


Figure 14. Structural parameters of the three-bar truss design problem.

Consider variable $\vec{y} = [y_1, y_2] = [A_1, A_2]$.

$$\text{Minimize}_{\vec{y}} \quad f(\vec{y}) = (2\sqrt{2}y_2 + y_2) \times l.$$

$$\begin{aligned} \text{Subject to} \quad g_1(\vec{y}) &= \frac{\sqrt{2}y_1 + y_2}{\sqrt{2}y_1^2 + 2y_1y_2} P - \sigma \leqslant 0. \\ g_2(\vec{y}) &= \frac{y_2}{\sqrt{2}y_1^2 + 2y_1y_2} P - \sigma \leqslant 0. \\ g_3(\vec{y}) &= \frac{y_2}{y_1 + \sqrt{2}y_2} P - \sigma \leqslant 0. \end{aligned} \quad (20)$$

Variable range $0 \leqslant y_1, y_2 \leqslant 1$.

Where $l = 10\text{cm}$, $P = 2\text{KN}/\text{cm}^2$, $\sigma = 2\text{KN}/\text{cm}^2$.

Table 14. Comparison of optimization results for the three-bar truss design problem.

Algorithm	Optimal Values for Variables		Optimal Weight
	A_1	A_2	
MOOA	0.788422741	0.4080882	263.8523476
OOA	0.801601097	0.372060283	263.9744812
AO	0.798247262	0.380200906	263.9637515
AOA	0.801494929	0.372319834	263.9726633
ChOA	0.788102737	0.409126196	263.8533748
HHO	0.790802975	0.401402021	263.8565027
GWO	0.788575469	0.407598478	263.8525933
RGWO	0.789695287	0.404498448	263.853552
MPSO	0.788584239	0.407642067	263.8523691

5.5. Tension/Compression Spring Design Problem

The tension/compression spring design problem aims to minimize the spring weight by optimizing three variables with four inequality constraints [48], as shown in Figure 15 and Equation (21). The decision variables are mean coil diameter (D), wire diameter (d), and the number of active coils (N).

Table 15 gives the optimal solutions of all algorithms in solving this problem. It is noted that the MOOA obtains the best results compared to other methods, and the minimum weight is 0.011174195.

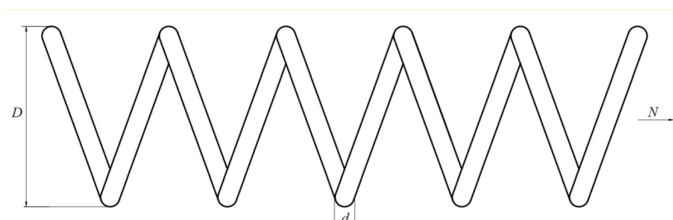


Figure 15. Structural parameters of the tension/compression spring design problem.

$$\begin{aligned}
\text{Consider variables} \quad & \vec{z} = [z_1, z_2, z_3] = [d, D, N]. \\
\text{Minimize} \quad & f(\vec{z}) = (z_3 + 2)z_2z_1^2 \\
\text{Subject to} \quad & g_1(\vec{z}) = 1 - z_2^3z_3 / (71785z_1^4) \leq 0. \\
& g_2(\vec{z}) = 4z_2^2 - z_1z_2 / 12566(z_2z_1^3 - z_1^4) + 1 / 5108z_1^2 - 1 \leq 0. \\
& g_3(\vec{z}) = 1 - 140.45z_1 / z_2^2z_3 \leq 0. \\
& g_4(\vec{z}) = (z_2 + z_1) / 1.5 - 1 \leq 0. \\
\text{Variable range} \quad & 0.05 \leq z_1 \leq 2. \\
& 0.25 \leq z_2 \leq 1.3. \\
& 2 \leq z_3 \leq 15.
\end{aligned} \tag{21}$$

Table 15. Comparison of optimization results for the tension/compression spring design problem.

Algorithm	Optimal Values for Variables			Optimal Weight
	d	D	N	
MOOA	0.05	0.355941091	10.55735374	0.011174195
OOA	0.060622644	0.677161681	3.122473338	0.012747993
AO	0.055901016	0.515478019	6.173513397	0.013166136
AOA	0.058981869	0.623069676	3.591682654	0.01212038
ChOA	0.059522545	0.640762158	3.425067068	0.012315867
HHO	0.059773263	0.649077517	3.350980104	0.012409203
GWO	0.058420246	0.605035817	3.775234562	0.011925525
RGWO	0.058714517	0.613346926	3.697405443	0.012046873
MPSO	0.05	0.373590618	10.15177501	0.011349473

6. Conclusions and Future Work

In this paper, an improved version of the osprey optimization algorithm, named the MOOA, is proposed for solving the global optimization problems. Three aspects of improvements have been made to the basic OOA. First is the Lévy flight strategy, which is used to expand the search range of hunting fish. And then the Brownian motion strategy is employed to increase the population's diversity and explore the promising regions. The last is the RFDB selection method, which is used to select individuals with high quality and identify the global optima. The experimental results of CEC2017 and CEC2022 test functions demonstrate that the proposed MOOA has superior performance compared to the other eight advanced optimization algorithms. Meanwhile, the results of the MOOA in five engineering design optimization problems also indicate that the MOOA has merit in real-world optimization problems. Therefore, the MOOA integrated with three improvement strategies is a powerful optimizer in solving these optimization problems, which can be used to solve more complex and challenging tasks.

Although the MOOA shows superiority in most test functions and some practical optimization problems, the MOOA still faces some drawbacks and can be enhanced further, such as the slow convergence speed on the unimodal function F1 of CEC2022. In addition, compared with other algorithms, the MOOA takes more computing time. Thus, the MOOA can be further improved by using other methods, such as a disturbance factor, or hybridizing with other optimization methods while not increasing the computational complexity. Future endeavors can also focus on applying the MOOA to solve more complex optimization problems, such as UAV path planning, feature selection, and scheduling problems.

Author Contributions: Conceptualization, L.Z. and X.L.; methodology, L.Z.; software, R.T.; validation, W.W. and G.J.; formal analysis, W.W.; investigation, G.J.; resources, X.L.; data curation, R.T.; writing—original draft preparation, L.Z. and X.L.; writing—review and editing, L.Z. and X.L.; visualization, R.T.; supervision, W.W. and G.J.; project administration, funding acquisition, X.L. All authors have read and agreed to the published version of the manuscript.

Funding: This research was funded by the China Postdoctoral Science Foundation, grant number 2020M681255.

Data Availability Statement: Data are available from the authors upon reasonable request.

Conflicts of Interest: The authors declare no conflicts of interest.

References

- Abdel-Basset, M.; Mohamed, R.; Zidan, M.; Jameel, M.; Abouhawwash, M. Mantis search algorithm: A novel bio-inspired algorithm for global optimization and engineering design problems. *Comput. Methods Appl. Mech. Eng.* **2023**, *415*, 116200. [[CrossRef](#)]
- Pham, Q.-V.; Mirjalili, S.; Kumar, N.; Alazab, M.; Hwang, W.-J. Whale optimization algorithm with applications to resource allocation in wireless networks. *IEEE Trans. Veh. Technol.* **2020**, *69*, 4285–4297. [[CrossRef](#)]
- Pekel, E. Solving technician routing and scheduling problem using improved particle swarm optimization. *Soft Comput.* **2020**, *24*, 19007–19015. [[CrossRef](#)]
- Abualigah, L.; Almotairi, K.H.; Elaziz, M.A. Multilevel thresholding image segmentation using meta-heuristic optimization algorithms: Comparative analysis, open challenges and new trends. *App. Intell.* **2023**, *53*, 11654–11704. [[CrossRef](#)]
- Hochbaum, D.S. Machine learning and data mining with combinatorial optimization algorithms. In *Recent Advances in Optimization and Modeling of Contemporary Problems*; INFORMS: Linthicum, MD, USA, 2018; pp. 109–129. [[CrossRef](#)]
- Ahmadianfar, I.; Haddad, O.B.; Chu, X. Gradient-based optimizer: A new metaheuristic optimization algorithm. *Inform. Sci.* **2020**, *540*, 131–159. [[CrossRef](#)]
- Ypma, T.J. Historical development of the newton-raphson method. *SIAM Rev.* **1995**, *37*, 531–551. [[CrossRef](#)]
- Kennedy, J.; Eberhart, R. Particle swarm optimization. In Proceedings of ICNN'95-International Conference on Neural Networks, Perth, WA, Australia, 27 November–1 December 1995; Volume 4, pp. 1942–1948. [[CrossRef](#)]
- Mirjalili, S.; Mirjalili, S.M.; Lewis, A. Grey wolf optimizer. *Adv. Eng. Softw.* **2014**, *69*, 46–61. [[CrossRef](#)]
- Abualigah, L.; Diabat, A.; Mirjalili, S.; Abd Elaziz, M.; Gandomi, A.H. The arithmetic optimization algorithm. *Comput. Methods Appl. Mech. Eng.* **2021**, *376*, 113609. [[CrossRef](#)]
- Wolpert, D.H.; Macready, W.G. No free lunch theorems for optimization. *IEEE Trans. Evol. Comput.* **1997**, *1*, 67–82. [[CrossRef](#)]
- Agushaka, J.O.; Ezugwu, A.E.; Saha, A.K.; Pal, J.; Abualigah, L.; Mirjalili, S. Greater cane rat algorithm (gcra): A nature-inspired metaheuristic for optimization problems. *Heliyon* **2024**, *10*, 31629. [[CrossRef](#)]
- Husseinzadeh Kashan, A. A new metaheuristic for optimization: Optics inspired optimization (oio). *Comput. Oper. Res.* **2015**, *55*, 99–125. [[CrossRef](#)]
- Yadav, A. Aefa: Artificial electric field algorithm for global optimization. *Swarm Evol. Comput.* **2019**, *48*, 93–108. [[CrossRef](#)]
- Talatahari, S.; Azizi, M.; Gandomi, A.H. Material generation algorithm: A novel metaheuristic algorithm for optimization of engineering problems. *Processes* **2021**, *9*, 859. [[CrossRef](#)]
- Farshchin, M.; Maniat, M.; Camp, C.V.; Pezeshk, S. School based optimization algorithm for design of steel frames. *Eng. Struct.* **2018**, *171*, 326–335. [[CrossRef](#)]
- Askari, Q.; Younas, I.; Saeed, M. Political optimizer: A novel socio-inspired meta-heuristic for global optimization. *Knowl. Based Syst.* **2020**, *195*, 105709. [[CrossRef](#)]
- Zhang, W.; Pan, K.; Li, S.; Wang, Y. Special forces algorithm: A novel meta-heuristic method for global optimization. *Math. Comput. Simul.* **2023**, *213*, 394–417. [[CrossRef](#)]
- Ong, K.M.; Ong, P.; Sia, C.K. A carnivorous plant algorithm for solving global optimization problems. *Appl. Soft Comput.* **2021**, *98*, 106833. [[CrossRef](#)]
- Zhao, S.; Zhang, T.; Ma, S.; Chen, M. Dandelion optimizer: A nature-inspired metaheuristic algorithm for engineering applications. *Eng. Appl. Artif. Intell.* **2022**, *114*, 105075. [[CrossRef](#)]
- Kaveh, M.; Mesgari, M.S.; Saeidian, B. Orchard algorithm (oa): A new meta-heuristic algorithm for solving discrete and continuous optimization problems. *Math. Comput. Simul.* **2023**, *208*, 95–135. [[CrossRef](#)]
- Holland, J.H. Genetic algorithms. *Sci. Am.* **1992**, *267*, 66–73. [[CrossRef](#)]
- Storn, R.; Price, K. Differential evolution—A simple and efficient heuristic for global optimization over continuous spaces. *J. Glob. Optim.* **1997**, *11*, 341–359. [[CrossRef](#)]
- Azizi, M.; Talatahari, S.; Gandomi, A.H. Fire hawk optimizer: A novel metaheuristic algorithm. *Artif. Intell. Rev.* **2023**, *56*, 287–363. [[CrossRef](#)]
- Dehghani, M.; Trojovsky, P. Osprey optimization algorithm: A new bio-inspired metaheuristic algorithm for solving engineering optimization problems. *Front. Mech. Eng.* **2023**, *8*, 1126450. [[CrossRef](#)]
- Abdel-Basset, R.; Mohamed, R.; Jameel, M.; Abouhawwash, M. Spider wasp optimizer: A novel meta-heuristic optimization algorithm. *Artif. Intell. Rev.* **2023**, *56*, 11675–11738. [[CrossRef](#)]
- Ismael, A.A.K.; Houssein, E.H.; Khafaga, D.S.; Abdullah Aldakheel, E.; AbdElrazek, A.S.; Said, M. Performance of the osprey optimization algorithm for solving economic load dispatch problem. *Mathematics* **2022**, *11*, 4107. [[CrossRef](#)]
- Zhao, J.; Gao, Z.-M.; Sun, W. The improved slime mould algorithm with levy flight. *J. Phys. Conf. Ser.* **2020**, *1617*, 012033. [[CrossRef](#)]
- Faramarzi, A.; Heidarinejad, M.; Mirjalili, S.; Gandomi, A.H. Marine predators algorithm: A nature-inspired metaheuristic. *Expert Syst. Appl.* **2020**, *152*, 113377. [[CrossRef](#)]

30. Duman, S.; Kahraman, H.T.; Guvenc, U.; Aras, S. Development of a levy flight and fdb-based coyote optimization algorithm for global optimization and real-world acopf problems. *Soft Comput.* **2020**, *25*, 6577–6617. [[CrossRef](#)]
31. Ma, C.; Huang, H.; Fan, Q.; Wei, J.; Du, Y.; Gao, W. Grey wolf optimizer based on aquila exploration method. *Expert Syst. Appl.* **2022**, *205*, 117629. [[CrossRef](#)]
32. Wu, G.; Mallipeddi, R.; Suganthan, P. Problem definitions and evaluation criteria for the cec 2017 competition and special session on constrained single objective real-parameter optimization. *Nanyang Technol. Univ. Singapore Tech. Rep.* **2016**, 1–18.
33. Yazdani, D.; Branke, J.; Omidvar, M.N.; Li, X.; Li, C.; Mavrovouniotis, M.; Nguyen, T.; Yao, X. IEEE CEC 2022 competition on dynamic optimization problems generated by generalized moving peaks benchmark. *arXiv* **2021**, arXiv:2106.06174.
34. Bouaouda, A.; Hashim, F.A.; Sayouti, Y.; Hussien, A.G. Pied kingfisher optimizer: A new bio-inspired algorithm for solving numerical optimization and industrial engineering problems. *Neural Comput. Appl.* **2024**, *36*, 15455–15513. [[CrossRef](#)]
35. Zhang, Q.; Bu, X.; Zhan, Z.; Li, J.; Zhang, H. An efficient optimization state-based coyote optimization algorithm and its applications. *Appl. Soft Comput.* **2023**, *147*, 110827. [[CrossRef](#)]
36. Abualigah, L.; Yousri, D.; Abd Elaziz, M.; Ewees, A.A.; Al-Qaness, M.A.; Gandomi, A.H. Aquila optimizer: A novel meta-heuristic optimization algorithm. *Comput. Ind. Eng.* **2021**, *157*, 107250. [[CrossRef](#)]
37. Khishe, M.; Mosavi, M.R. Chimp optimization algorithm. *Expert Syst. Appl.* **2020**, *149*, 113338. [[CrossRef](#)]
38. Heidari, A.A.; Mirjalili, S.; Faris, H.; Aljarah, I.; Mafarja, M.; Chen, H. Harris hawks optimization: Algorithm and applications. *Future Gen. Comput. Syst.* **2019**, *97*, 849–872. [[CrossRef](#)]
39. Banaie-Dezfouli, M.; Nadimi-Shahraki, M.H.; Beheshti, Z. R-gwo: Representative-based grey wolf optimizer for solving engineering problems. *Appl. Soft Comput.* **2021**, *106*, 107328. [[CrossRef](#)]
40. Bao, G.; Mao, K. Particle swarm optimization algorithm with asymmetric time varying acceleration coefficients. In Proceeding of the 2009 IEEE International Conference on Robotics and Biomimetics (ROBIO), Guilin, China, 19–23 December 2009; pp. 2134–2139.
41. Friedman, M. The use of ranks to avoid the assumption of normality implicit in the analysis of variance. *J. Am. Stat. Assoc.* **1937**, *32*, 675–701. [[CrossRef](#)]
42. Wilcoxon, F. *Individual Comparisons by Ranking Methods*; Springer: New York, NY, USA, 1992; pp. 196–202. [[CrossRef](#)]
43. Zhong, R.; Yu, J.; Munetomo, Z.M. Srime: A strengthened rime with latin hypercube sampling and embedded distance-based selection for engineering optimization problems. *Neural Comput. Appl.* **2024**, *36*, 6721–6740. [[CrossRef](#)]
44. Deb, K. Optimal design of a welded beam via genetic algorithms. *AIAA J.* **1991**, *29*, 2013–2015. [[CrossRef](#)]
45. Kannan, B.K.; Kramer, S.N. An augmented lagrange multiplier based method for mixed integer discrete continuous optimization and its applications to mechanical design. *J. Mech. Des.* **1994**, *116*, 405–411. [[CrossRef](#)]
46. Hu, G.; Zheng, Y.; Abualigah, L.; Hussien, A.G. Detdo: An adaptive hybrid dandelion optimizer for engineering optimization. *Adv. Eng. Inform.* **2023**, *57*, 102004. [[CrossRef](#)]
47. Sadollah, A.; Bahreininejad, A.; Eskandar, H.; Hamdi, M. Mine blast algorithm: A new population based algorithm for solving constrained engineering optimization problems. *Appl. Soft Comput.* **2013**, *13*, 2592–2612. [[CrossRef](#)]
48. Belegundu, A.D., Arora, J. A study of mathematical programming methods for structural optimization. Part II: Numerical results. *Int. J. Numer. Methods Eng.* **1985**, *21*, 1601–1623. [[CrossRef](#)]

Disclaimer/Publisher’s Note: The statements, opinions and data contained in all publications are solely those of the individual author(s) and contributor(s) and not of MDPI and/or the editor(s). MDPI and/or the editor(s) disclaim responsibility for any injury to people or property resulting from any ideas, methods, instructions or products referred to in the content.